Selected Paper

Thermostable Rh Catalysts Supported on Metal Phosphates: Effect of Aging on Catalytic Activity for NO–CO–C_3H_6–O_2 Reactions

Keita Ikeue, Kyosuke Murakami, Satoshi Hinokuma, Kosuke Uemura, Dongjie Zhang, and Masato Machida*

Department of Nano Science and Technology, Graduate School of Science and Technology, Kumamoto University, 2-39-1 Kurokami, Kumamoto 860-8555

Received September 28, 2009; E-mail: machida@kumamoto-u.ac.jp

The catalytic activity and thermostability of Rh catalysts (0.4% loading) have been studied using various metal phosphates (B, Al, Ga, Y, La, Pr, Zr, and Ce) as support materials. Temperature-programmed reactions of mixtures of NO, CO, C_3H_6, and O_2 with the stoichiometric A/F ratio (14.6) exhibited a steep rise in conversion efficiency as a common feature of Rh supported on metal phosphates. The activity of $Rh/AlPO_4$ was found to be the highest even after aging at 900 °C for 25 h in a stream of 10% H_2O/air. Among four types of $AlPO_4$ polymorphs having different BET surface area, i.e, berlinite ($5\,m^2\,g^{-1}$), cristobalite ($1\,m^2\,g^{-1}$), tridymite ($82\,m^2\,g^{-1}$), and microporous $AlPO_4$-5 ($330\,m^2\,g^{-1}$), tridymite $AlPO_4$ achieved the lowest light-off temperature. The slow grain growth of tridymite $AlPO_4$ at $\leq$1000 °C is a possible reason for the stability against sintering, whereas one-dimensional micropores of $AlPO_4$-5 are unstable in the high-temperature steam.

Currently, more than 80% of the world Rh demand is for use in three-way catalysts for gasoline-fueled automobiles.[1–5] Rh is thus among the scarcest of precious metals that needs a substantial thrift. Although precious metals including Rh are highly dispersed in a fresh automotive catalyst, they are gradually agglomerated into large grains with a low surface area and hence a low catalytic activity in a long period of operation. To counter this effect, conventional automotive catalysts have been loaded with an excess amount of precious metal, ensuring that the performance meets the present car emission standards. Now, the strategies to construct more stable catalysts requiring less precious metal loadings, especially for the very expensive Rh, are of paramount importance.

We have recently reported that aluminum orthophosphate ($AlPO_4$) becomes a robust support material producing optimum interactions with Rh species, which can reduce the threshold loading, owing to the high thermal stability and the high dispersion of Rh species anchored onto the surface.[6] The outstanding stability was demonstrated by thermal aging at 900 °C for 500 h in a stream of water vapor, where conventional Rh loaded on La-modified γ-Al_2O_3 (La–Al_2O_3) totally lost its catalytic activity. Another feature to be noted is the very low threshold Rh loading ($\leq$0.01%), which corresponds to about one twentieth of a conventional $Rh/La–Al_2O_3$ catalyst.

$AlPO_4$ materials have been studied extensively not only as a catalyst but also as a catalyst support for organic synthesis, polymerization and/or decomposition of chlorofluorocarbons.[7,8] Interestingly however, $AlPO_4$ has been considered an unfavorable material in the area of automotive applications, because it can be found in used catalysts that are deactivated through phosphorous poisoning. Phosphorous species originate from engine oil additives, zinc dialkyldithiophosphate (ZDDP), and are deposited as phosphates on the catalyst surface. The dense and stable overlayers thus formed cause pore blockage, loss of surface area, and occlusion of active precious metals.[9–11] The phosphate in part reacts with porous Al_2O_3 support to form $AlPO_4$ and further reactions with an oxygen storage material, CeO_2, to yield $CePO_4$, are pointed out to destroy the oxygen storage function.[12,13] For these reasons, aluminum phosphate has not been studied as a material for autocatalysts to the best of our knowledge.

We have pointed out that the benefits of this material extend to thermal and chemical stabilities. $AlPO_4$ possesses a high melting point of about 2000 °C, suitable for high-temperature applications. A weak acidity at the surface is expected not only to have the catalytic activity of precious metal catalysts, but also to suppress the catalyst deactivation caused by the adsorption of sulfur oxides (SO_x). The new support $AlPO_4$ in combination with Rh is thus useful for the design and synthesis of thermostable automotive catalysts containing less precious metal. However, the use of other metal phosphates has not been examined in detail.

In the present work, we have studied Rh catalysts supported on various metal phosphate materials to study their catalytic performance and thermostability in comparison with those of conventional metal oxide supports. The catalytic activity for simulated stoichiometric automobile exhaust containing NO, CO, C_3H_6, and O_2 with a stoichiometric A/F ratio (14.6) has been evaluated after thermal aging. Because $AlPO_4$ has polymorphic forms including berlinite, cristobalite, tridymite-types and several zeolite structures, their suitability as catalyst supports for Rh was also studied with the aim of finding optimum support materials for Rh.

Experimental

Catalyst Preparation. $AlPO_4$ was prepared from $Al(NO_3)_3$

Published on the web February 18, 2010; doi:10.1246/bcsj.20090256

Table 1. BET Surface Area of Supports and Catalytic Activity of 0.4% Rh Catalysts

Support		S_{BET}[a]/$m^2\,g^{-1}$		$T_{50\%}$[b]/°C		
		Before aging	After aging	NO	CO	C_3H_6
$AlPO_4$	—	82	45	315	315	315
La_2O_3–Al_2O_3	3 wt % La_2O_3	126	85	350	330	370
FeO–Al_2O_3	Fe/Al = 1.0	10	<1	490	495	520
MgO–Al_2O_3	Mg/Al = 3.0	168	107	420	410	450
MgO	—	78	18	>600	>600	>600
TiO_2	—	50	<1	>600	>600	>600
SiO_2	—	304	225	385	385	385
FSM-16	—	993	83	>600	380	410
Pr-FSM-16	Pr/Si = 0.12	720	68	390	400	390
ZrO_2	—	38	11	365	340	380
Nd_2O_3–ZrO_2	15 mol % Nd_2O_3	62	40	360	370	400
CeO_2	—	157	9	470	235	380
CoO–CeO_2	Co/Ce = 1.0	65	5	>600	510	320
MnO–CeO_2	Mn/Ce = 0.33	80	16	510	325	315
NiO–CeO_2	Ni/Ce = 0.33	60	3	>600	430	600
MnO–PrO_x	Mn/Pr = 0.33	15	5	>600	450	460
CoO–PrO_x	Co/Pr = 0.33	12	6	>600	340	570
FeO–PrO_x	Fe/Pr = 0.33	15	3	>600	>600	>600

a) BET surface area of supports. b) Temperature at which NO conversion reaches 50%. Aging: 10% H_2O/air, 900 °C, 25 h, catalytic reaction: 0.050% NO, 0.510% CO, 0.039% C_3H_6, 0.400% O_2, and He balance, $W/F = 5.0 \times 10^{-4}$ g min cm^{-3}.

(Wako Pure Chemicals Ind. Ltd., 99.9%) and H_3PO_4 (Wako Pure Chemicals Ind. Ltd., 85%) as follows. A solution of 0.05 mol of H_3PO_4 in 50 mL of deionized water was added dropwise to a solution containing 0.05 mol of $Al(NO_3)_3$ in 50 mL of deionized water with vigorous stirring. Then, an aqueous ammonia solution (25%) was added dropwise until the pH of the supernatant was 4.5. The white gel thus obtained was recovered by filtration and washed with deionized water several times. After being dried in air at 100 °C, the solid thus obtained was calcined in air at 1000 °C for 5 h to yield $AlPO_4$ with tridymite structure ($S_{BET} = 82\,m^2\,g^{-1}$). The same procedure was also applied to the synthesis of phosphates of B, Ga, Y, La, Pr, Zr, and Ce. Other phases of aluminum phosphates such as low cristobalite $AlPO_4$ and zeolite $AlPO_4$-5, were prepared according to the literature.[14,15] Commercially available berlinite $AlPO_4$ was also used as a reference (Alfa Aesar, 97%).

Rh-loaded on $AlPO_4$ (0.4% as Rh metal) was prepared by impregnation of an aqueous solution of $Rh(NO_3)_3$, followed by drying in air (100 °C), air calcination (600 °C, 3 h). Rh catalysts supported on other metal phosphates, La–Al_2O_3 (3% La_2O_3 added γ-Al_2O_3), MgO, SiO_2, TiO_2, ZrO_2, CeO_2, and their binary oxides were also prepared in a similar way. The neat oxides were supplied by the Catalysis Society of Japan and their S_{BET} values are listed in Table 1.

Characterization and Catalytic Tests. Powder X-ray diffraction (XRD) measurement was performed on the product using monochromated Cu Kα radiation (30 kV, 20 mA, Rigaku Multiflex). The content of Rh was determined by X-ray fluorescence measurement (Rigaku EDXL300). Metal dispersion and particle size of Rh was measured by CO chemisorption using a commercial instrument (Bel-cat, Bel Japan, Inc.) at 50 °C after reduction at 400 °C in H_2. Direct observation by TEM (FEI TECNAI F20, 200 kV) was also performed to check the consistency with the CO chemisorption measurement. BET surface area (S_{BET}) was calculated from N_2 adsorption measured at 77 K (Belsorp, Bel Japan, Inc.). Temperature-programmed reduction (TPR) of Rh catalysts was conducted in a fixed-bed quartz tube under 1 vol % H_2 in He with a heating rate of 10 °C min^{-1} from room temperature to 600 °C.

Prior to the catalytic test, Rh-loaded catalysts were pretreated in a stream of 10% H_2O/air at 900 °C for 25 h. Catalytic tests were carried out in a flow reactor at atmospheric pressure. 50 mg of catalyst (10–20 mesh) was fixed in a quartz tube (4 mm i.d.) by quartz wool at both ends of the catalyst bed. Temperature dependence of catalytic activity was evaluated by heating the catalyst bed from room temperature to 600 °C at a constant rate of 10 °C min^{-1} while supplying a simulated exhaust gas mixture containing NO (0.050%), CO (0.510%), C_3H_6 (0.039%), O_2 (0.400%), and He (balance) supplied at 100 $cm^3\,min^{-1}$ ($W/F = 5.0 \times 10^{-4}$ g min cm^{-3}, SV = 2×10^4–$6 \times 10^4\,h^{-1}$). The gas composition corresponds to the stoichiometric air-to-fuel ratio ($A/F = 14.6$). The effluent gas was analyzed using a Pfeiffer GSD30101 mass spectrometer and a Horiba VA3000 NDIR gas analyzer.

Results and Discussion

Screening of Thermally Stable Support Materials for Rh. A viable catalyst needs to achieve light-off at low temperatures for start-up and to sustain activity at temperatures as high as 900 °C. In the case of Rh catalysts, a metallic Rh forming under a reducing atmosphere has a higher melting point than Pt and Pd and is rather stable against sintering. However, high-temperature aging in excess O_2 causes deactivation by sintering and interactions between Rh oxide and oxide supports.[2,5,16–18] Our catalytic test in the present study was therefore carried out after aging catalysts at 900 °C for 25 h in a stream of 10% H_2O in air. Table 1 summarizes the catalytic activity of Rh catalysts (0.4% loading) supported on various materials for the conversion of CO, NO, and C_3H_6. The light-off temperature is expressed in terms of $T_{50\%}$, which is the temperature as 50% conversions of NO, CO, and/or C_3H_6 are achieved.

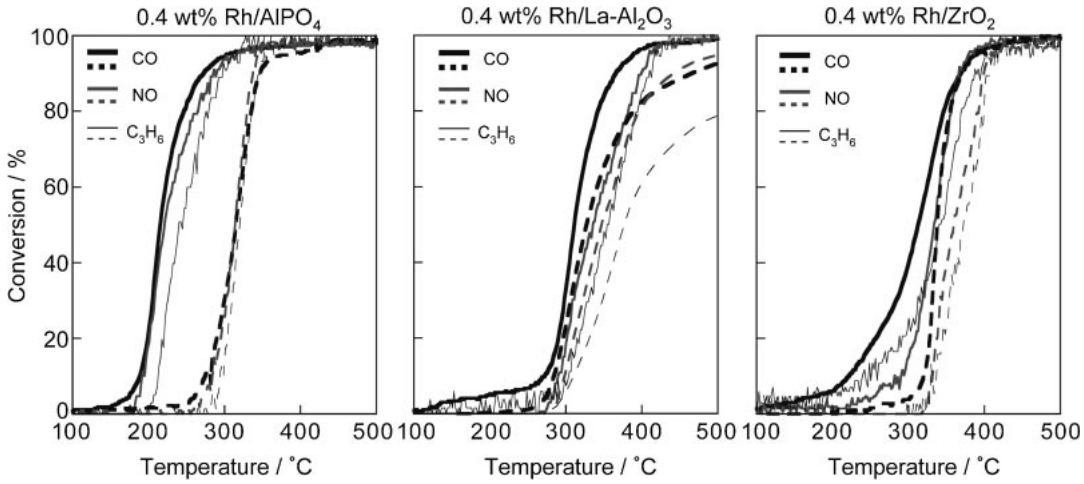

Figure 1. Light-off curves for NO–CO–C_3H_6–O_2 reaction over 0.4% Rh-loaded $AlPO_4$, La–Al_2O_3, and ZrO_2 before (solid lines) and after (dashed lines) thermal aging. The catalyst (0.05 g) was heated at the constant rate of 10 °C min^{-1} in a stream of gaseous mixtures of 0.050% NO, 0.510% CO, 0.039% C_3H_6, 0.400% O_2, and He balance supplied at 100 cm^3 min^{-1} ($W/F = 5.0 \times 10^{-4}$ g min cm^{-3}). The catalyst was aged in a stream of 10% H_2O/air at 900 °C for 25 h prior to the catalytic test.

Table 2. BET Surface Area of Catalysts and Particle Size of Rh before and after Aging (10% H_2O/Air, 900 °C, 25 h)

Catalyst	S_{BET}/m^2 g^{-1}		Rh particle size/nm	
	Before aging	After aging	Before aging	After aging
0.4% Rh/$AlPO_4$[a)]	63	41	3.3[b)]	—
			4.7[c)]	7.2[c)]
0.4% Rh/La–Al_2O_3[a)]	121	71	1.7[b)]	112[c)]
0.4% Rh/ZrO_2[a)]	38	5	14[b)]	5.1[b)]

a) Calcined at 600 °C for 3 h in air. b) Determined by CO chemisorption. c) Mean particle size determined by TEM observation of 100 particles of Rh species.

Light-off of a stream of NO, CO, and C_3H_6 is observed at the low temperature of 315 °C for $AlPO_4$, whereas almost all the conventional oxide supports require more than 350 °C. Among the oxide supports, La–Al_2O_3 and ZrO_2 show relatively lower light-off temperatures. Therefore, their temperature dependences of conversion efficiencies are compared with $AlPO_4$ in Figure 1 before and after the thermal aging at 900 °C in 10% H_2O/air. Before the aging, Rh/$AlPO_4$ initiated the reaction at the lowest temperature of ≤200 °C and reached complete conversion at around 300 °C. The thermal aging caused the light-off shifting about 100 °C toward higher temperatures, but the steep rise of conversion efficiencies within a narrow temperature range remained unchanged. Table 2 lists S_{BET} and Rh particle size of these supported Rh catalysts. Here, the particle sizes for the as-prepared catalysts are calculated from the CO chemisorption, which could not be applied to aged Rh/$AlPO_4$ and Rh/La–Al_2O_3 catalysts, probably because the interaction with supports inhibited the adsorption of CO onto Rh. The small amount of loading (0.4%) was not enough for detection by XRD measurement. In such cases, the mean particle size was obtained from the size distribution of Rh particles in TEM images (Supporting Information). This gave a value (4.7 nm) for Rh/$AlPO_4$ larger than the value obtained by chemisorption (3.3 nm), but they are enough for the rough evaluation of the particle growth. The aging of Rh/$AlPO_4$ decreased S_{BET} from 63 to 41 m^2 g^{-1}, but the mean Rh particle size was still less than 10 nm (Table 2). This is consistent with our previous results,[6] which demonstrated that the high activity of Rh/$AlPO_4$ could be preserved even after longer thermal aging (900 °C, 500 h), which caused a significant deactivation of Rh/La–Al_2O_3.

La–Al_2O_3 has been mostly used as a support for automotive catalysts. The addition of La is to suppress the sintering of Al_2O_3 due to the thermally activated phase transformation from γ- to α-Al_2O_3.[19,20] Nevertheless, the deactivation was observed as the difference in conversion efficiencies between as prepared (solid lines) and aged (dotted lines) catalysts in Figure 1, which became more obvious at higher reaction temperatures. As shown in Table 2, TEM observation suggested the significant sintering of Rh particles more than expected from Figure 1. The catalyst after 25-h aging contained a number of large agglomerates (>200 nm) consisting of Rh–Al oxides together with much smaller Rh particles of less than 20 nm. The result of catalytic test should therefore be affected by the broad distribution of Rh size. But, after aging at this temperature (900 °C) for 500 h, almost all the Rh forms large agglomerates with a negligible activity as reported in our previous paper.[6] Thermal deactivation of Rh/Al_2O_3 has frequently been pointed out,[2,5,16,17] when the aging is carried out at temperature higher than 600 °C in the presence of O_2. A number of explanations have been proposed for the deactivation, including dissolution of Rh oxide into Al_2O_3, formation of Rh aluminate ($RhAlO_x$), encapsulation of Rh by Al_2O_3, and other strong interactions.[18,21–23]

ZrO_2 is also well-known as a component of automotive catalysts because of its stability over a wide temperature range and resistance to catalytic poisoning. As shown in Figure 1, the light-off temperature of Rh/ZrO_2 was increased by the thermal aging, but complete conversion was still achieved at ≤400 °C. Thus, ZrO_2 is an excellent support for Rh. In spite of sintering of ZrO_2 after the aging, the particle size of Rh decreased from 14 to 5 nm (Table 2), which could also be confirmed by TEM

observation. This may imply the occurrence of redispersion caused by the reversible Rh–ZrO_2 interaction by treating the catalyst in an oxidizing atmosphere, but the mechanism of this phenomenon is not clear at this stage. A similar redispersion of Pt on CeO_2 has recently been studied in detail by Nagai et al.[24]

Among the other materials in Table 1, an amorphous SiO_2 also exhibited a high activity. By contrast, mesoporous silica (FSM-16) did not become a suitable support because of the thermal instability. Rh/CeO_2 initiated CO oxidation at very low temperature ($T_{50\%} = 235\,°C$), but the activity for NO and C_3H_6 was not enough. Binary systems including CeO_2 could not improve the catalytic activity.

As was evident from a simple comparison of three catalysts in Figure 1, the high activity of Rh/$AlPO_4$ should be noted. The Rh species should be in the form of oxide after air calcination at 600 °C. The reducibility of Rh oxide species on each as prepared and aged catalysts was measured by means of H_2-TPR, which gave the maximum rate of H_2 consumption based on reduction of Rh species in the following sequence of increasing temperatures; $AlPO_4$ (123 °C) < ZrO_2 (145 °C) < La–Al_2O_3 (294 °C). After thermal aging, the H_2 consumption for Rh/$AlPO_4$ and Rh/ZrO_2 was shifted to 154 and 338 °C, respectively, but Rh/La–Al_2O_3 did not show clearly H_2 consumption up to 600 °C. These results indicate that the reduction of Rh oxide to form active metallic Rh is considered to be a key factor for the low light-off temperature shown in Figure 1. As in the case for Rh/La–Al_2O_3, thermal aging yields Rh oxide species having larger particle sizes and/or stronger interactions with supports, resulting in less reducibility and thus a shift of the light-off to higher temperatures. By contrast, Rh oxide did not cause solid-state reactions with $AlPO_4$. Non-reactive but strong anchoring effect is a possible reason for the thermal stability of highly-dispersed Rh nanoparticles on $AlPO_4$. As shown in our previous report,[6] the superiority of Rh/$AlPO_4$ over oxide-supported Rh catalysts is found to be more obvious at lower loading amounts of Rh (≤0.2%).

Rh Catalyst Supported on Metal Phosphates. Other metal phosphate materials having high melting points (>1400 °C) were next studied as supports for Rh. Figure 2 shows the light-off curves for NO in the NO–CO–C_3H_6–O_2 reaction over 0.4% Rh-loaded metal phosphates. $AlPO_4$ showed the largest value of S_{BET} before and after aging, whereas other metal phosphates showed much smaller values (Table 3). Nevertheless, all the metal phosphates showed a steep rise of conversion efficiency as was observed for Rh/$AlPO_4$. The light-off temperature is dependent on the type of metal phosphates, increasing in the sequence of Al < Y < Zr < Ce < Ga < La < B. With an exception of Al and Y cases, the catalytic reactions over phosphate supports tend to be retarded at high conversion efficiencies. The different catalytic activity may result from surface area, acid–base properties, and/or structural factors of metal phosphates. The Rh/$AlPO_4$ catalyst with the highest catalytic activity and the largest S_{BET} is thus promising for practical applications.

Structure and Thermal Stability of $AlPO_4$. The merit of Rh/$AlPO_4$ is the high catalytic activity and thermal stability suitable for high-temperature applications. Here, the reported phase relation and crystal structure of $AlPO_4$ is briefly described for latter discussion. According to the phase diagram

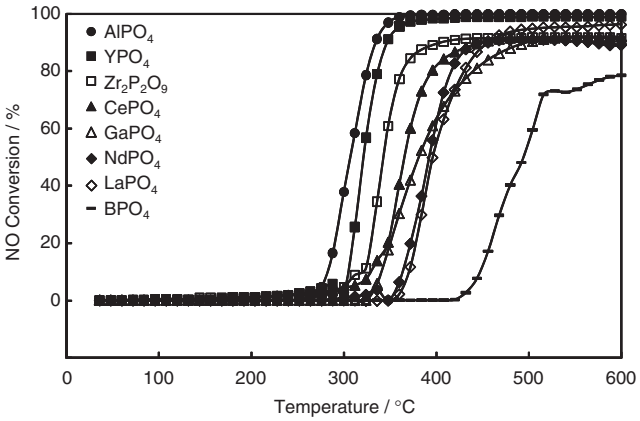

Figure 2. Light-off curves for NO in NO–CO–C_3H_6–O_2 reaction over 0.4% Rh catalysts supported on various metal phosphates. The catalytic test and catalyst aging were conducted as described in Figure 1.

Table 3. BET Surface Area of Metal Phosphates

	$S_{BET}/m^2\,g^{-1}$	
	Before aging[a)]	After aging[b)]
BPO_4	10	9
$AlPO_4$	82	45
$GaPO_4$	17	12
YPO_4	8	3
$Zr_2P_2O_9$	3	3
$LaPO_4$	3	3
$CePO_4$	3	3
$NdPO_4$	1	1

a) Calcined at 1000 °C for 5 h in air. b) Aging at 900 °C for 25 h in 10% H_2O/air.

of Al_2O_3–P_2O_5,[25] an equimolar compound, $AlPO_4$, is a thermodynamically stable phase with a high melting point of about 2000 °C in contrast to the volatile P_2O_5. $AlPO_4$ exists in three different polymorphs, i.e., berlinite, tridymite, and cristobalite, which are well known as SiO_2 analogs.[26–28] They all consist of AlO_4 and PO_4 tetrahedral units and each P atom shares an oxygen atom with each of four adjacent Al atoms and vice versa to form four connected 3D networks. The stability relation among these polymorphs is summarized as follows:[27] berlinite (≤700 °C) < tridymite (≤1050 °C) < cristobalite.

However, the phase relation is influenced by the starting materials, preparation procedures, calcination conditions as well as additives.[26–28] Besides these dense phases, microporous $AlPO_4$ phases have also been synthesized by hydrothermal technique.[15]

Figure 3 shows the XRD patterns and S_{BET} of present $AlPO_4$ product after heating at elevated temperatures. The precipitation forming from $Al(NO_3)_3$, H_3PO_4, and NH_4OH at pH 4.5 yielded an equimolar solid (P/Al = 1) with an amorphous structure, which transformed into a tridymite phase after calcination at ≥900 °C. Very weak diffraction peaks observed after calcination at ≤1000 °C are indicative of a low crystalline phase with a large S_{BET} (80–100 $m^2\,g^{-1}$) and a very slow grain growth in the temperature range. By contrast, the diffraction peaks became intense after the calcination at >1000 °C, where

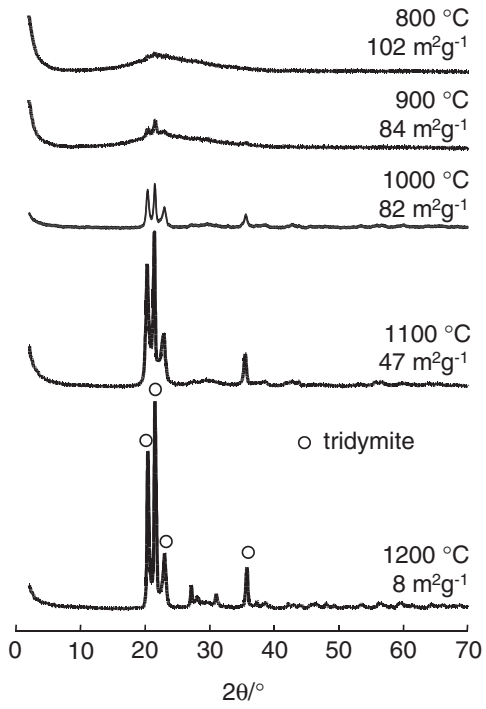

Figure 3. XRD patterns and BET surface areas of $AlPO_4$ after calcination at elevated temperatures.

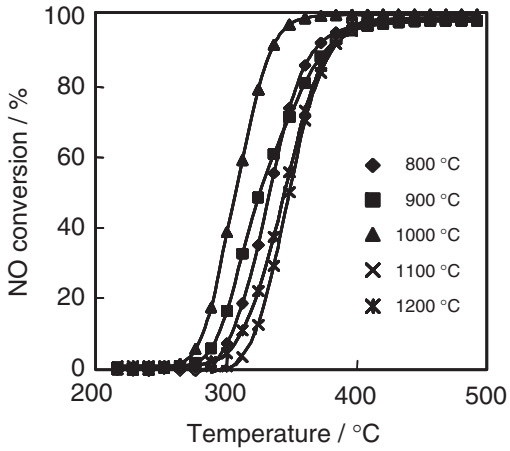

Figure 4. Light-off curves for NO in NO–CO–C_3H_6–O_2 reaction over 0.4% Rh catalysts supported on tridymite type $AlPO_4$ after calcination at elevated temperatures. The catalytic test and catalyst aging were conducted in the same way described in Figure 1.

a steep loss of S_{BET} was observed. The phase transformation to the cristobalite could not be observed at $\leq$1200 °C, which is not consistent with the phase relation described above.

Figure 4 shows the NO conversion in the NO–CO–C_3H_6–O_2 reaction over 0.4% Rh loaded on $AlPO_4$ with different calcination temperatures (800–1200 °C). The reaction rate determined at 280 °C (NO conversion less than 20%) is not correlated with S_{BET} of $AlPO_4$; the highest activity was observed for $AlPO_4$ after calcination at 1000 °C. When using a large surface area $AlPO_4$ calcined at low temperature $\leq$900 °C, Rh loading followed by thermal aging at 900 °C

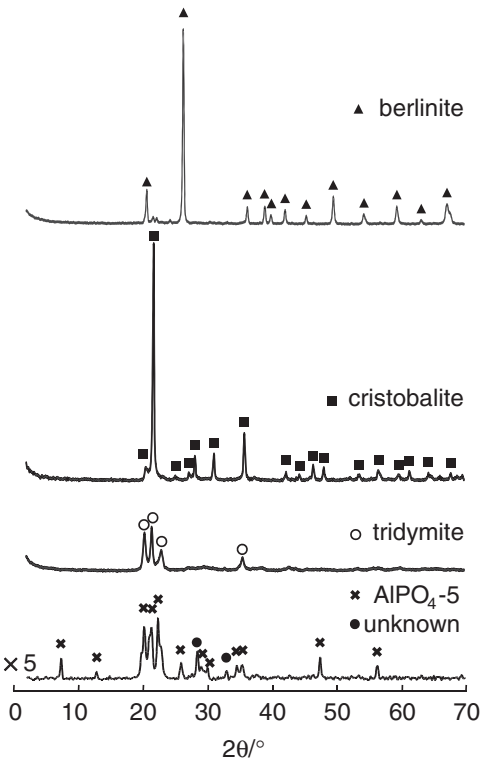

Figure 5. XRD patterns of four different types of $AlPO_4$ phases after calcination at 1000 °C.

should cause significant sintering and crystallization of $AlPO_4$, which is accompanied by grain growth and/or encapsulation of Rh species. By contrast, Rh loaded on $AlPO_4$ calcined at 1000 °C should be free of such deterioration in thermal aging. This is a possible reason for the highest activity when $AlPO_4$ after calcination at 1000 °C was used as a support. The P/Al ratios of all the calcined $AlPO_4$ were equal to unity before and after use in the catalytic test. Unlike the other low-surface area phosphates (B, Ga, Zr, La, and Ce) shown in Figure 2, the retardation of reaction in the high conversion region was not obvious even after calcination at 1200 °C ($S_{BET} = 8\,m^2\,g^{-1}$). These results may be explained by the efficient light-off characteristics of Rh loaded on $AlPO_4$ as above described (Figure 1).

Catalytic Activity of Rh Supported on Different $AlPO_4$. Since our previous work has been focused on tridymite $AlPO_4$, Rh catalysts were next prepared using other $AlPO_4$ phases having a cristobalite, berlinite, and zeolite $AlPO_4$-5 structure. Figure 5 and Table 4 show the XRD and S_{BET}, respectively, of these $AlPO_4$ polymorphs after air calcination at 1000 °C. Although the three dense phases of tridymite-, cristobalite-, and berlinites $AlPO_4$ preserved their original crystal structure, microporous $AlPO_4$-5 was partially decomposed. Impregnation of Rh was thus applied to $AlPO_4$-5 calcined at 550 °C ($S_{BET} = 330\,m^2\,g^{-1}$). Unlike the tridymite, very sharp and strong diffraction peaks of the cristobalite and berlinite phases suggest a high crystallinity. This is consistent with the fact that the S_{BET} of berlinite ($5\,m^2\,g^{-1}$) and cristobalite ($1\,m^2\,g^{-1}$) were much smaller than tridymite ($82\,m^2\,g^{-1}$) as shown in Table 4. The slow grain growth of tridymite $AlPO_4$ at $\leq$1000 °C would be a reason for the higher thermal stability.

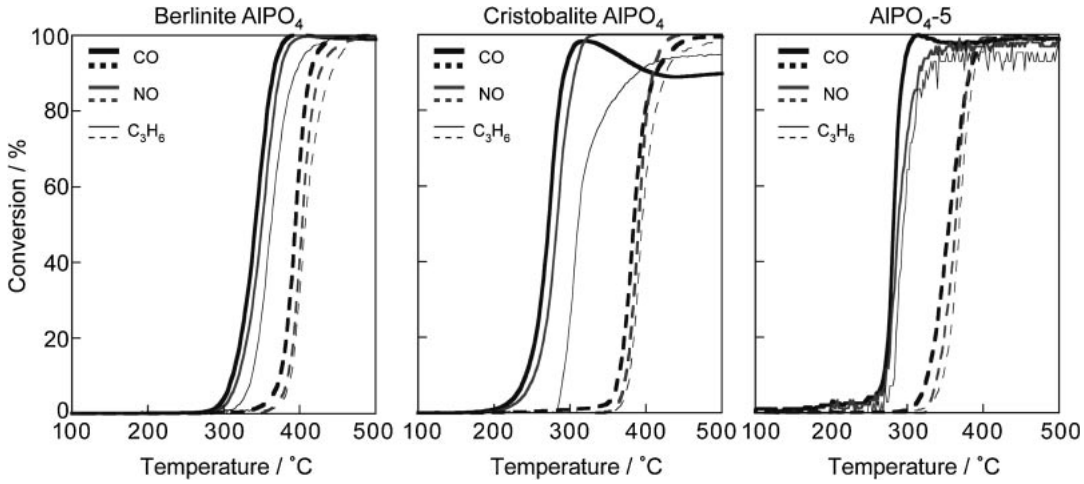

Figure 6. Light-off curves for NO–CO–C_3H_6–O_2 reaction over 0.4% Rh loaded on $AlPO_4$ polymorphs before (solid lines) and after (dashed lines) thermal aging. The catalytic test and catalyst aging were conducted in the same way described in Figure 1.

Table 4. BET Surface Area of $AlPO_4$ Polymorphs before and after Aging

	S_{BET}[a]/$m^2\,g^{-1}$	
	Before aging	After aging
Tridymite[b]	82	45
Berlinite[b]	5	4
Cristobalite[b]	1	2
$AlPO_4$-5[c]	330	160

a) BET surface area of support. Aging: 10% H_2O/air, 900 °C, 25 h. b) Calcined at 1000 °C for 5 h in air. c) Calcined at 550 °C for 5 h in air.

The light-off curves for NO–CO–C_3H_6–O_2 reaction over 0.4% Rh loaded on these $AlPO_4$ polymorphs are shown in Figure 6. A simple comparison with Figure 1 demonstrates that none of these other $AlPO_4$ phases exhibits catalytic activity and stability superior to that of tridymite $AlPO_4$. The light-off temperatures ($T_{50\%}$) exhibit the following sequences of increasing values: tridymite < cristobalite < $AlPO_4$-5 < berlinite for as prepared catalysts and tridymite < $AlPO_4$-5 < cristobalite ≈ berlinite, after the thermal aging. The aging did not affect the low surface area of cristobalite and/or berlinite $AlPO_4$ phases (Table 4), but the sintering of Rh on both supports seems to be faster than on tridymite $AlPO_4$. Actually, the metal dispersions of Rh on cristobalite and berlinite measured by CO chemisorption were less than 3%. To cancel the effect of support surface area, it is useful to compare the activities of the catalysts in Figure 6 and Rh loaded on tridymite $AlPO_4$ after calcination at 1200 °C (Figure 4, $S_{BET} = 8\,m^2\,g^{-1}$). However, the higher activity of the latter was found to be still obvious.

As prepared Rh/$AlPO_4$-5 was less active than Rh loaded on tridymite $AlPO_4$. This is rationalized by the assumption that most of the reactions occurring on Rh/$AlPO_4$-5 take place on the external surface. Actually, our TEM observation demonstrated that Rh was mainly deposited on external surface of $AlPO_4$-5 to give the lower metallic dispersion (16%). Moreover, the aging of $AlPO_4$-5 caused a significant loss of S_{BET} ($330 \rightarrow 160\,m^2\,g^{-1}$), which was caused by partial collapse of the zeolite structure to unknown dense phases (Figure 5). Such a structural deterioration would also give rise to the deactivation by encapsulation of Rh species.

The reason for the higher catalytic activity of Rh on tridymite $AlPO_4$ is not clear at this stage, but it may be associated with the structural similarity between tridymite (hexagonal, $P6_3mc$, $a = 0.510$ nm)[29] and Rh_2O_3 (rhombohedral, $R\bar{3}c$, $a = 0.513$ nm).[30] Because of similar ionic arrangement in their (001) faces, tridymite $AlPO_4$ is expected to form a coherent interface with Rh_2O_3. According to TEM observation in our previous study,[6] RhO_x presents as a thin plate spreading over the $AlPO_4$ surface, which proves the strong interaction to stabilize RhO_x against coalescence during high-temperature aging. Further structural analysis is now under investigation to elucidate the relationships among the structure of RhO_x/$AlPO_4$ interface, catalytic activity, and thermal stability.

Conclusion

The present study has demonstrated that Rh catalysts loaded on metal phosphates exhibit catalytic activity and thermal stability under air aging conditions. Among metal phosphates, tridymite $AlPO_4$ achieves the lowest light-off temperature for a simulated gas stream corresponding to stoichiometric A/F ratio. The slow grain growth of the tridymite $AlPO_4$ in comparison with other $AlPO_4$ polymorphs plays a key role in the outstanding thermal stability. Thermal stability of Rh/$AlPO_4$ in excess O_2 is promising, because gasoline engine technology is now directed toward lean-burn operation to reduce fuel consumption and CO_2 emission. Because the aging and catalytic tests of the present work do not cover the broad range of oxidizing, reducing, and stoichiometric gas compositions found in automotive catalyst operation, additional studies will be needed to assess the suitability of Rh/$AlPO_4$. In particular, our study is now extended not only to a lean-burn condition but also in the wide range of gas compositions with dynamic rich-lean cycles that real catalysts are exposed to under vehicle driving conditions.

This study was supported by Elements Science and Technology Project from the Ministry of Education, Culture, Sports, Science and Technology. The authors thank Drs.

Maorong Chai, Yunosuke Nakahara, and Takahiro Sato (Mitsui Mining and Smelting Co., Ltd.) for many helpful discussions on the stability of phosphate supports.

Supporting Information

Details on TEM photographs and Rh particle size distribution for $Rh/AlPO_4$ and $Rh/La–Al_2O_3$ before and after aging. This material is available free of charge on the web at http://www.csj.jp/journals/bcsj/.

References

1 D. Jollie, *Platinum 2008*, Johnson Matthey, Roystone, Hertfordshire, **2008**, p. 4.

2 R. M. Heck, R. J. Farrauto, S. T. Gulati, *Catalytic Air Pollution Control*, 3rd ed., John Willey & Sons, Hoboken, New Jersey, **2009**.

3 M. Shelef, *Catal. Rev.—Sci. Eng.* **1975**, *11*, 1.

4 K. C. Taylor, *Catal. Rev.—Sci. Eng.* **1993**, *35*, 457.

5 H. S. Gandhi, G. W. Graham, R. W. McCabe, *J. Catal.* **2003**, *216*, 433.

6 M. Machida, K. Murakami, S. Hinokuma, K. Uemura, K. Ikeue, M. Matsuda, M. Chai, Y. Nakahara, T. Sato, *Chem. Mater.* **2009**, *21*, 1796.

7 J. B. Moffat, *Catal. Rev.—Sci. Eng.* **1978**, *18*, 199.

8 Y. Takita, M. Ninomiya, H. Miyake, H. Wakamatsu, Y. Yoshinaga, T. Ishihara, *Phys. Chem. Chem. Phys.* **1999**, *1*, 4501.

9 W. B. Williamson, J. Perry, H. S. Gandhi, J. L. Bomback, *Appl. Catal.* **1985**, *15*, 277.

10 M. L. Granados, C. Larese, F. C. Galisteo, R. Mariscal, J. L. G. Fierro, R. Fernández-Ruíz, R. Sanguino, M. Luna, *Catal. Today* **2005**, *107–108*, 77.

11 D. M. Fernandes, A. A. Neto, M. J. B. Cardoso, F. M. Z. Zotin, *Catal. Today* **2008**, *133–135*, 574.

12 M. J. Rokosz, A. E. Chen, C. K. Lowe-Ma, A. V. Kucherov, D. Benson, M. C. Paputa Peck, R. W. McCabe, *Appl. Catal., B* **2001**, *33*, 205.

13 L. Xu, G. Guo, D. Uy, A. E. O'Neill, W. H. Weber, M. J. Rokosz, R. W. McCabe, *Appl. Catal., B* **2004**, *50*, 113.

14 M. Sato, E. Kobayashi, M. Matsumoto, S. Matsuda, *Rev. Chim. Miner.* **1985**, *122*, 37.

15 S. T. Wilson, B. M. Lok, C. A. Messina, T. R. Cannan, E. M. Flanigen, *J. Am. Chem. Soc.* **1982**, *104*, 1146.

16 H. C. Yao, S. Japar, M. Shelef, *J. Catal.* **1977**, *50*, 407.

17 H. C. Yao, H. K. Stepien, H. S. Gandhi, *J. Catal.* **1980**, *61*, 547.

18 D. D. Beck, T. W. Capehart, C. Wong, D. N. Belton, *J. Catal.* **1993**, *144*, 311.

19 R. M. Levy, D. J. Bauer, *J. Catal.* **1967**, *9*, 76.

20 H. Schaper, E. B. M. Doesburg, L. L. Van Reijen, *Appl. Catal.* **1983**, *7*, 211.

21 C. Wong, R. W. McCabe, *J. Catal.* **1989**, *119*, 47.

22 J. G. Chen, M. L. Colaianni, P. J. Chen, J. T. Yates, Jr., G. B. Fisher, *J. Phys. Chem.* **1990**, *94*, 5059.

23 R. W. McCabe, R. K. Usmen, K. Ober, H. S. Gandhi, *J. Catal.* **1995**, *151*, 385.

24 Y. Nagai, K. Dohmae, Y. Ikeda, N. Takagi, T. Tanabe, N. Hara, G. Guilera, S. Pascarelli, M. A. Newton, O. Kuno, H. Jiang, H. Shinjoh, S. Matsumoto, *Angew. Chem., Int. Ed.* **2008**, *47*, 9303.

25 I. V. Tananaev, E. V. Maksimchuk, Yu. G. Bushuev, S. A. Shestov, *Inorg. Mater.* **1978**, *14*, 562.

26 J. M. Bennett, W. J. Dytrych, J. J. Pluth, J. W. Richardson, Jr., J. V. Smith, *Zeolites* **1986**, *6*, 349.

27 R. Debnath, J. Chaudhuri, *J. Solid State Chem.* **1992**, *97*, 163.

28 S. N. Achary, O. D. Jayakumar, A. K. Tyagi, S. K. Kulshresththa, *J. Solid State Chem.* **2003**, *176*, 37.

29 H. A. Graetsch, *Acta Crystallogr., Sect. C* **2001**, *57*, 665.

30 J. M. D. Coey, *Acta Crystallogr., Sect. B* **1970**, *26*, 1876.